A Vulnerability Map of a Commercial Aircraft

Y. I. Moon, G. Bharatram, Capt. S. A. Schimmels, Dr. V. B. Venkayya
Structures Division, WL/FIBAD
Bldg. 45, Area B
Wright Patterson AFB, Ohio 45433-7552

ABSTRACT

A method of developing a vulnerability map of a commercial aircraft is presented using MSC/DYTRAN and MSC/NASTRAN. The intent of the map is to establish the vulnerability of every point in the cargo hold where a bomb can explode. One might interpret each point in the cargo bay as having four dimensions. Three are spatial coordinates and the fourth is the maximum size of the bomb the structure can withstand without catastrophic failure. The vulnerability of the aircraft is examined from two distinct failure scenarios. The first is the response immediately after the bomb explosion. The second is the subsequent flight to the nearest airport for safe landing. The immediate response analysis is determined with MSC/DYTRAN and the post explosion analysis is made by MSC/NASTRAN. A complete vulnerability map requires many failure scenarios and a large number of MSC/DYTRAN and MSC/NASTRAN analyses. Six points in the cargo hold were critically examined to demonstrate the concept.

1. Introduction

The vulnerability of commercial airplanes has drawn a lot of attention due to the increased activities of terrorists who have brought down a number of airplanes over the past years, resulting in loss of life, property damage and general disruptions. The Federal Aviation Administration sponsored a number of static tests (on the ground) using both B-52 bombers and old B-707 commercial aircraft to understand the behavior of explosion inside an aircraft. Although the B-52 is a single compartment aircraft, the tests using them provided valuable information on pressure propagation and reflection after explosion. The B-52 structure is also representative of a typical semi-monocoque construction used in commercial aircraft. Most of the tests in the commercial aircraft were conducted in the cargo compartment.

Enhancing aircraft survivability needs to start with an understanding of what happens when an explosive device detonates in an airplane. An airframe is a very complex structure designed for high efficiency, while operating under severe dynamic environments at low margins of safety. Thus, it is important to know the failure sequence of structural components due to an in-flight explosion. The failure sequence helps to determine the safety of airplanes under these assumed flying conditions. The vulnerability of an aircraft to internal explosions inside the cargo compartment depends on the charge size, its location, and on the flight condition.

The purpose of this paper is to outline an empirical method for estimation of the vulnerability of the commercial aircraft when a bomb explodes in the cargo hold. The explosion scenario in an aircraft in flight is extremely complex and many intractable factors can affect the outcome. This investigation addresses two important aspects of the explosion scenario:

(a) the state of the aircraft immediately after explosion, and

(b) if the aircraft survives, the post-explosion flight to the nearest airport for safe landing.

Both of these issues play a critical role in developing a vulnerability map of the commercial aircraft cargo hold. If the size of the bomb is large enough and is placed at a critical location, catastrophic failure of the aircraft is imminent. Then two questions arise: (a) how large is large enough?, and (b) where is the critical location in the cargo hold?.

The concept of a vulnerability map is a sort of a strategy to clarify rather than answering precisely these questions. It is based on a proposition that each point in the cargo hold can be assigned four dimensions. Three coordinates are to locate its position and the fourth is the maxi-

mum size of the bomb that can be exploded at this point without catastrophic failure of the aircraft.

Assuming such a vulnerability map can be developed successfully, it can be used to compare with the smallest bomb that can be detected by state-of-the-art inspection devices. If there is an overlap between the largest bomb tolerance of the structure and the smallest bomb detection capability in any part of the cargo hold, it can be considered safe area. The rest of the area of the cargo hold, where there is no overlap, is open for development of strategy that involves:

a) hardening the airframe to increase the tolerance,

b) allocating the area to better inspected baggage, and

c) designing special cargo containers for this area.

In the forgoing discussion it was tacitly assumed that we have the wherewithal to determine the largest bomb that a given location in the structure can take without catastrophic failure. This is no easy task. Nevertheless, this paper presents a plausible solution to the problem. It involves:

(a) an assumed failure criteria,

(b) evaluation of the structure immediately after explosion, and

(c) post explosion flight.

Evaluation of the immediate damage involves MSC/DYTRAN models. The post explosion flight predictions are based on global models using MSC/NASTRAN.

Section 2 contains both physical and analytical descriptions of the B-707 forward fuselage section. Generation of finite element models are explained in Section 3. Section 4 describes steps to generate vulnerability maps and presents vulnerability maps while Section 5 summarizes the analytical investigation.

2. Description of the Aircraft

The aircraft chosen for the analysis was the Boeing 707-300 and -400 series. A brief description of the aircraft structure is provided in this section. A more detailed description of the aircraft is available in References [1,2]. The primary source of information for the aircraft was the four volume stress reports [3] which contain the structural substantiation of both forward and aft fuselage for the Boeing 707-300 and 400 series airplanes. The reports contain fuselage loads, brief analysis of the basic monocoque structure, description of the major structural components of the fuselage, and some fuselage section properties. Stiffener and skin data are given at body stations where there are significant changes in structure. The most useful source of information was an actual forward fuselage section shown in Figure 1. Figure 1 shows a view of a B-707 forward fuselage cross-section, where outer skin with stringers attached are clearly seen. The passenger floor in the middle divides the cross-section into two sections: the upper portion for passengers and the lower portion for the cargo. Transverse frames of both passenger and cargo floor are shown with holes for electrical control cables. The liner is connected to the outer skin via stringers. The insulation material fills the space between the liner and the outer skin. Figure 2 shows a typical cross-section of a B-707 forward fuselage which was used to construct finite element models and can basically be constructed by two circles: one has a radius of 74 inches and the other 67.1 inches.

The outer skins are laid on these circles. The longitudinal splices of the fuselage skin are lap-jointed along the body direction and riveted circumferentially. The thickness of skin varies from 0.04 to 0.07 inch. Typical material for fuselage skins is aluminum clad 2024-T3 or T4.

The outer skin is reinforced by stringers which are placed along the axial direction and by the circumferential frames. Typical stringers are aluminum 7075 rolled hat sections and typical frames are aluminum 7075 rolled “Z” sections across the upper crown, with a formed web and angle section on the sides and around the bottom.

Skins are connected to neighboring skins either by lap joints or butt joints. Figure 3 shows locations of butt and lap joints at body stations.

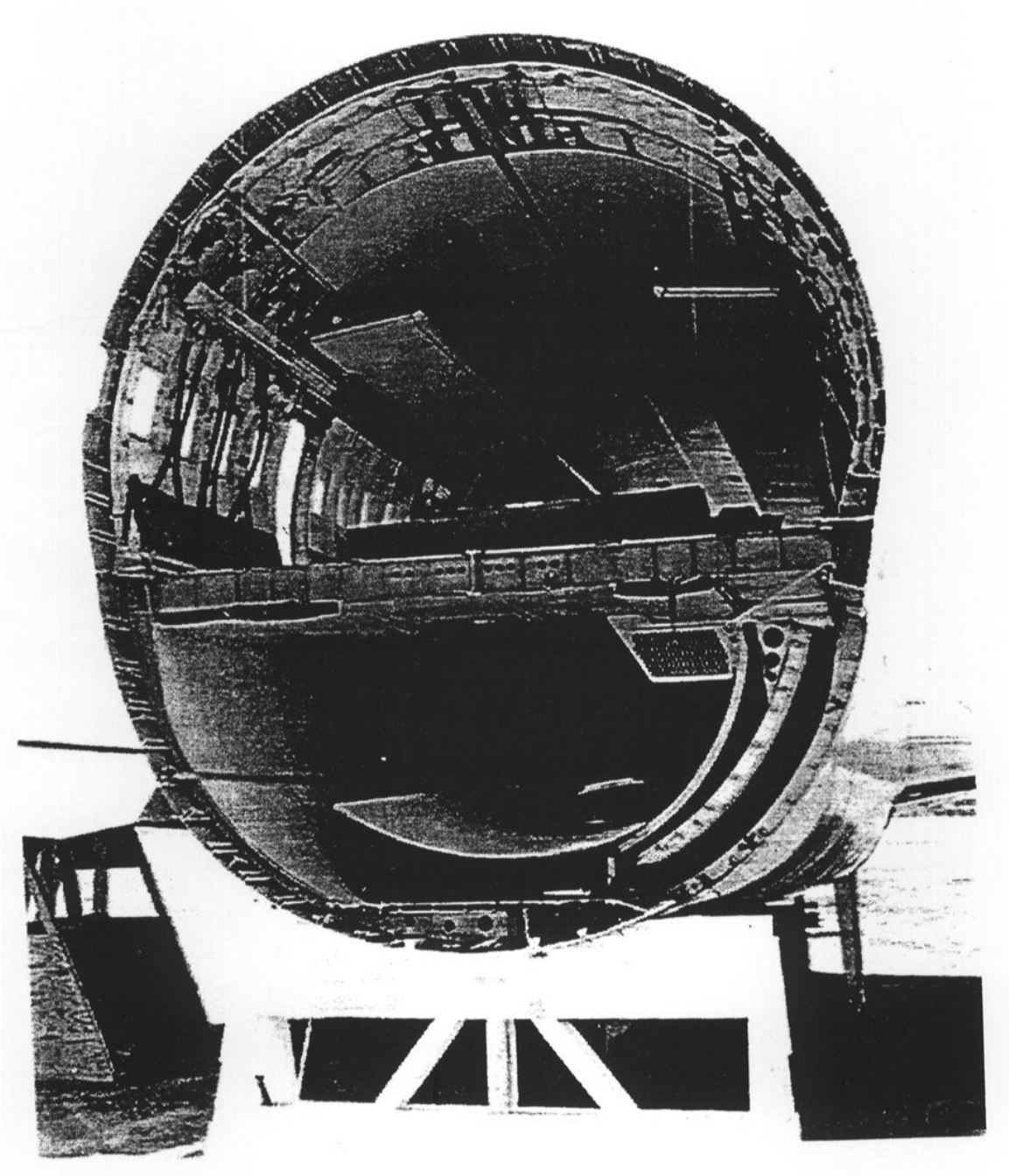

Figure 1. B-707 Forward Fusalage Cross-section

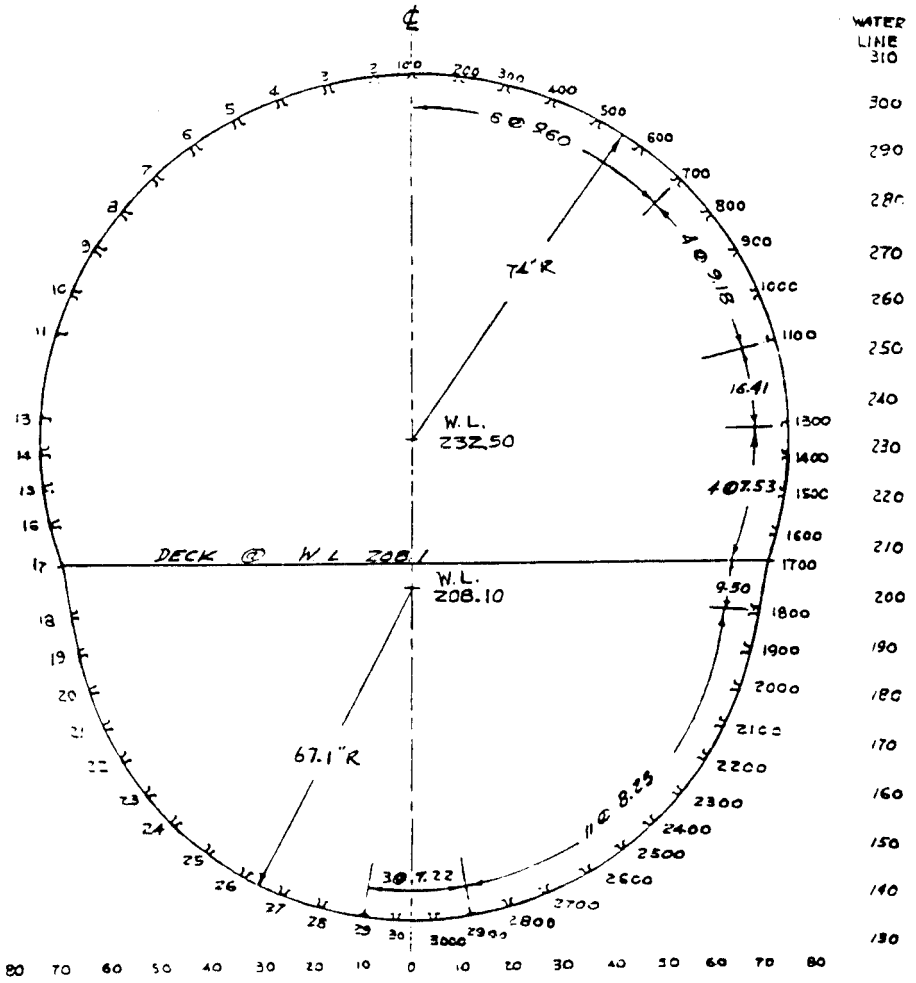

Figure 2. Typical Cross-section with Stiffener

There are two floors in the forward fuselage. The passenger floor is located at Stringer 17 which is at waterline 208.10 inches, and the cargo floor is at Stringer 27 which is at waterline 141.5 inches. The passenger floor divides the fuselage into an upper chamber for passengers and a lower chamber for cargo. The passenger floor has transverse floor beams spaced 20 inches apart and each beam is supported by a body frame through a shear connection.

The cargo bay consists of the passenger floor on the top, a cargo floor at the bottom, right and left side walls, bulkheads at both ends, and a cargo door at the right. They are shown in Figure 3. The cargo floor is a relatively rigid member, and consists of thick panels and transverse and longitudinal stiffeners.

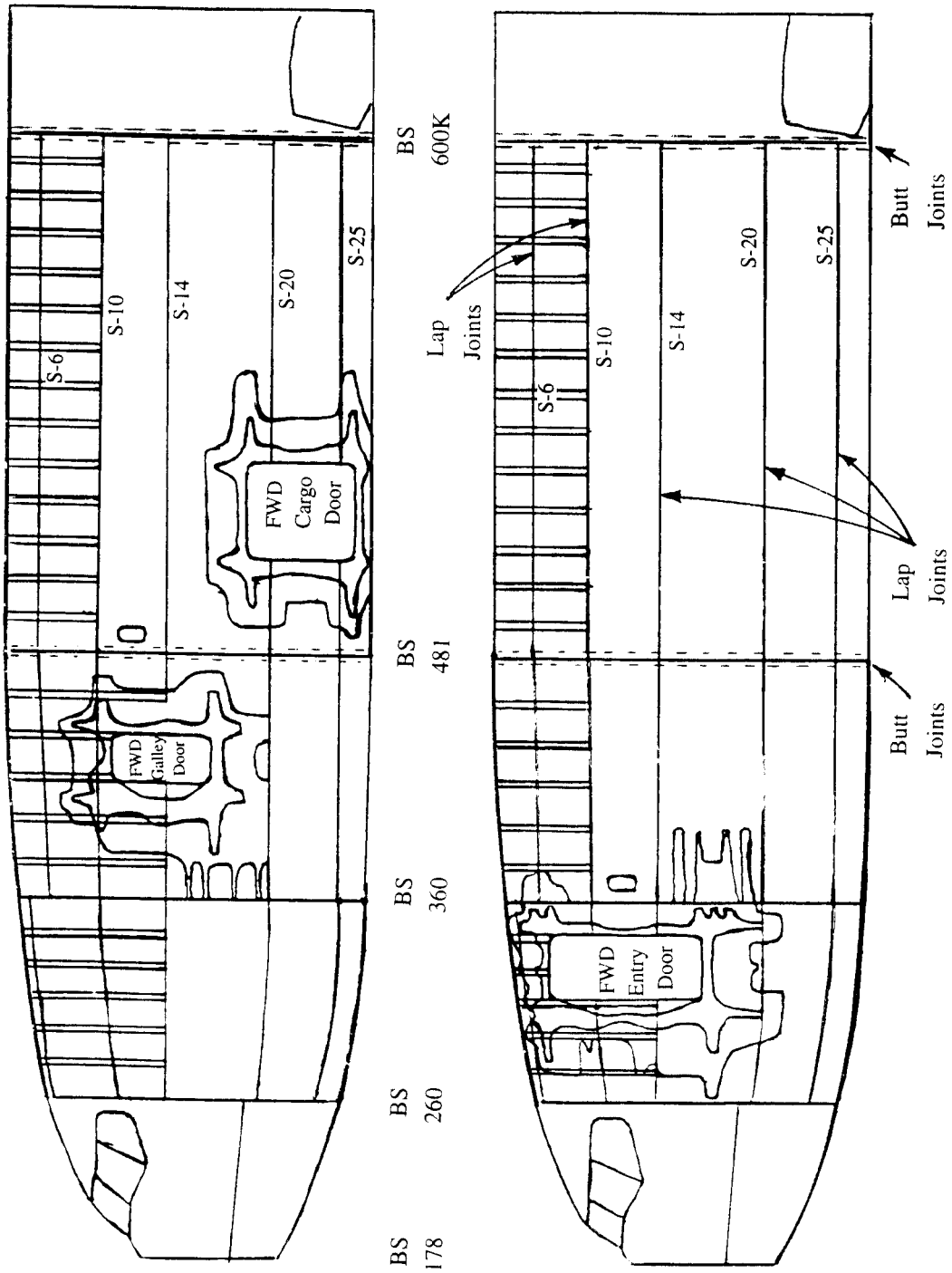

Figure 3. Butt and Lap Joint Locations on Boeing 707 Forward Fuselage

3. Description of Finite Element Models

This section covers the generation of finite element models used for the analysis. As the blast tests were conducted by placing the charge in the forward fuselage of the cargo compartment, only the forward fuselage section was modeled for the construction of the vulnerability map. An MSC/NASTRAN model was used to study the overall behavior of the aircraft after the explosion and MSC/DYTRAN model was used to investigate the immediate response of the structures to internal blast.

3.1 MSC/NASTRAN (Global) Model

The global finite element model employs two types of elements available in NASTRAN; bar and plate elements. There are ten different types of bars used for circumferential frames and 17 different types for stringers. CBAR elements are also used to model both longitudinal and transverse floor (passenger and cargo) stiffeners, stiffeners at bulkheads, passenger window frames, and door (cargo and passenger) frames.

The plate element in MSC/NASTRAN can be used to model membranes, plates, and thick or thin shells. Skins, passenger and cargo floors, walls at BS 400 and BS 600 H, and bulkheads are modeled with plate elements (CQUAD4 and CTRIA3).

The finite element model shown in Figure 4 has become a base line model for the analysis and construction of the vulnerability map.

For the boundary conditions, the model is assumed to be cantilevered at BS 600K. All the grid points at the bulkhead (BS 600K) are constrained in all directions, since it is known that the airplane in flight deflects with respect to the roots of the wing because of the heavy structure in the body around the wing roots. The effect of the cockpit on the model is accounted for by taking the total mass (COMN2) of the cockpit at the CG of the cockpit and connecting the mass to the grids at BS 360 by rigid bars (RBE3). The finite element model consists of 4,508 GRIDs, 5,044 CBARs, and 4,880 plate elements (CQUAD4 & CTRIA3). This model was employed for analyzing global effects on the aircraft such as overall stress/strain distribution, deformation pattern and generating a vulnerability map. The overall behavior of the aircraft for post explosion flight was simulated using the global model.

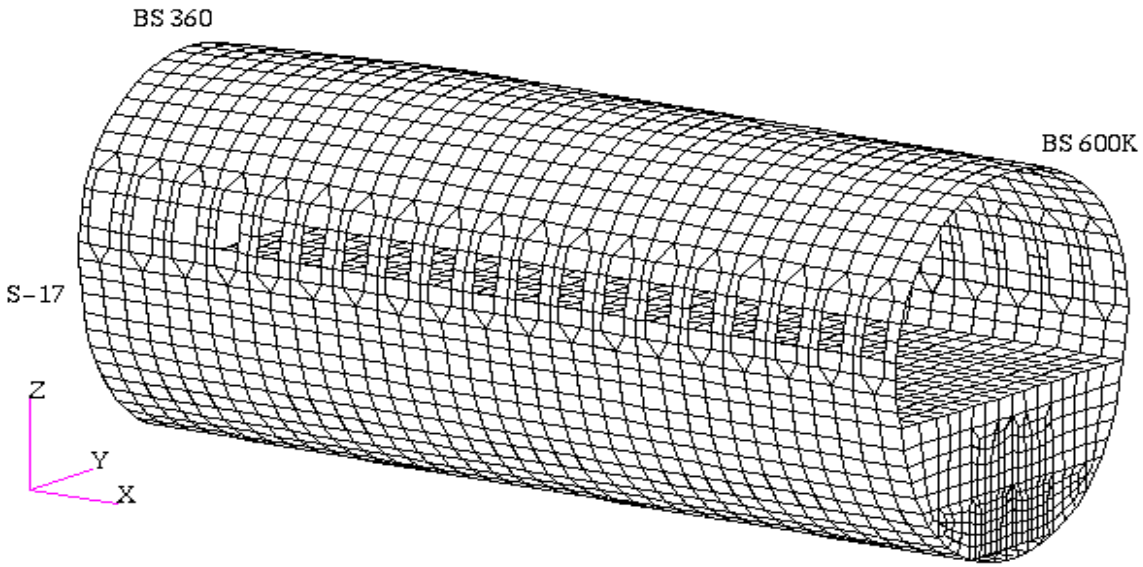

(a) Hidden Line Plot

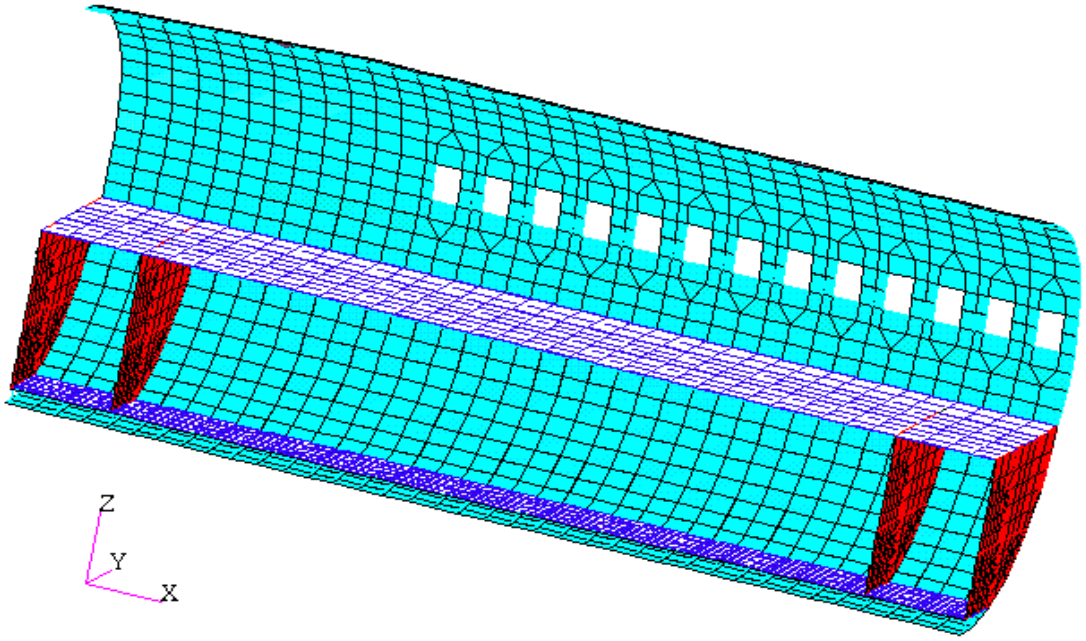

(b) Finite Element Model Plot
(Exposing right-hand side)

Figure 4. Finite Element Model of Forward Fuselage

3.2 MSC/DYTRAN Model

The MSC/DYTRAN global model of the forward fuselage cargo bay was constructed to study the fluid-structure interactions due to an internal explosion in the cargo compartment. This model was also used to validate the NASTRAN base line finite element model, using the test data generated by the Aircraft Loading Test (ALT) series conducted on B-707 aircrafts, using a series of charges placed at different locations. This global model was run on MSC/DYTRAN [4] which simulates the interaction of fluid and structure and uses two main processors. The Lagrangian processor uses structural finite elements (i.e., NASTRAN bulk data deck), and the Eulerian processor uses solid elements representing fluid (air in the model). To interact the two processors, the ALE (Arbitrary Lagrange-Euler) coupling was chosen. The Lagrangian and Eulerian nodes in the ALE interface surface coincide in physical space but are distinct in logical space. In other words, nodes in the Lagrangian model, Eulerian model and ALE surface should be unique, and all elements should have distinct ID numbers. There are other restrictions in making the Eulerian solid model, which include: (1) the size of solid elements surrounding the charge needs to be small enough that the sphere representing the charge contains at least four solid elements (the smallest solid element is one cubic inch); (2) the ratio of change of length with neighboring solid elements is supposed to be 20% or less; and (3) the maximum number of solid elements to share the same node is eight.

In modeling the interaction of a high explosive with the surrounding material (air in this case), the shape of the charge was modeled as a sphere of dense, hot gas with the correct mass and energy of the explosive charge.

3.2.1 MSC/DYTRAN Model I (charge at BS600)

This model has a C-4 charge placed at the center of the core cross-section (at BS 600). Lagrange model shown in Figure 5 is constructed based on the NASTRAN model in Figure 4, and the elements in the core area between BS 580 and BS 620 where the charge is located are doubled for better results. At the present time the DYTRAN code is not capable of handling any solid barrier such as the passenger floor which divides the fuselage into two closed volumes: passenger compartment and cargo bay. Thus any structural barrier existing between the fluid (air in this case) and the outer structure was eliminated. The MSC/DYTRAN model does not include the passenger cabin, and structures under the cabin floor. Excluded also from the model are both

chambers: one is the avionics bay at the front end (from BS 360 to BS 400), and the other is for environmental control system which is located at the rear end (from BS 600H to BS 600K). Therefore the final MSC/DYTRAN finite element model covers only the cargo bay from BS 400 to BS 600H between passenger and cabin floors.

The Eulerian model has 19,885 nodes and 21,192 HEXA elements. This Eulerian model was meshed in two ways; a regular mesh and a dense mesh. A dense mesh was applied for the core area, ranging from BS 580 to BS 620, which includes the place of the charge and its vicinity, and a regular mesh for all the areas other than the core. In regular meshing, the size of solid elements (CHEXA) in the Eulerian model is kept constant longitudinally while in dense meshing the size becomes bigger in both longitudinal and transverse directions starting with the solid elements of a cubic inch size at the center of the core portion. Figure 5 shows the section cuts in longitudinal (section A-A) and transverse (sections 1-1 & 2-2) directions to expose the cross-sections. Figure 6 is the left-half of the Eulerian model of Figure 5 when it is cut along the middle longitudinal line A-A, thus exposing the core section where the charge is placed. The side view of the MSC/DYTRAN model I is shown in Figure 7(a). Figure 7(b) is the side view of the MSC/DYTRAN model II. Figure 7 (c) shows the regular vertical transverse cross-section (section 2-2).

Figures from 7(d), 8(a), and 8(b) show the transverse sections for the three locations (Section 1-1). Three models were generated for this location marked by “x”, where the charge is placed. One at the aircraft centerline which is 60” (Location 1 in Figure 7(d)) from the outer skin, the second at 30” (Location 2 in Figure 8(a)) from the outer skin and the third 15” (Location 3 in Figure 8(b) from the outer skin.

3.2.2 MSC/DYTRAN Model II (charge at BS600F)

A Lagrangian and Eulerian model was generated for a charge placed at BS 600F (Figure 7(b)). This location is 40 inches away from the wing root bulkhead. The only difference between model I and model II is the core portion of both the Lagrangian and Eulerian model. The core portion was translated by 60 inches toward the wing root in model II. The three charge locations remain unchanged in a transverse direction (y-coordinates of three locations). As the charge was placed near the wing root it was presumed that the vulnerability of the aircraft would increase and significant failure of the stringers would be observed.

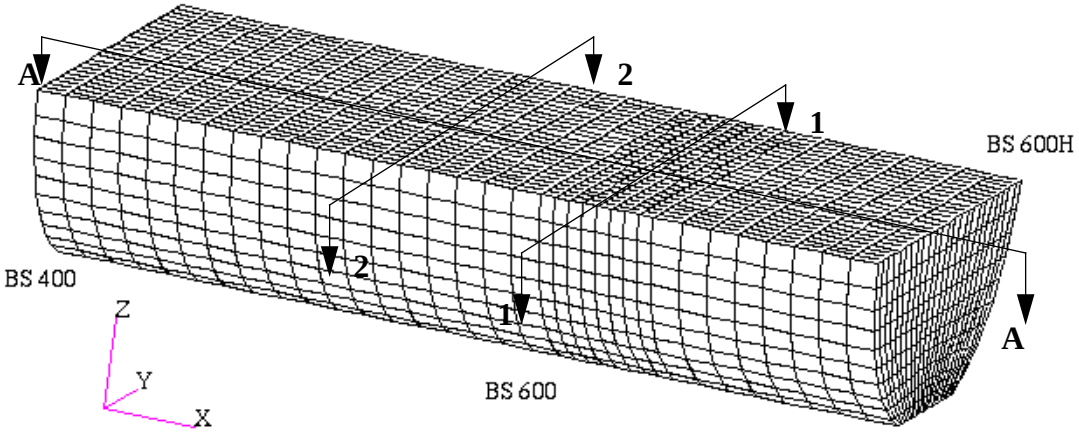

Figure 5. Eulerian Model with Cut-section Designation

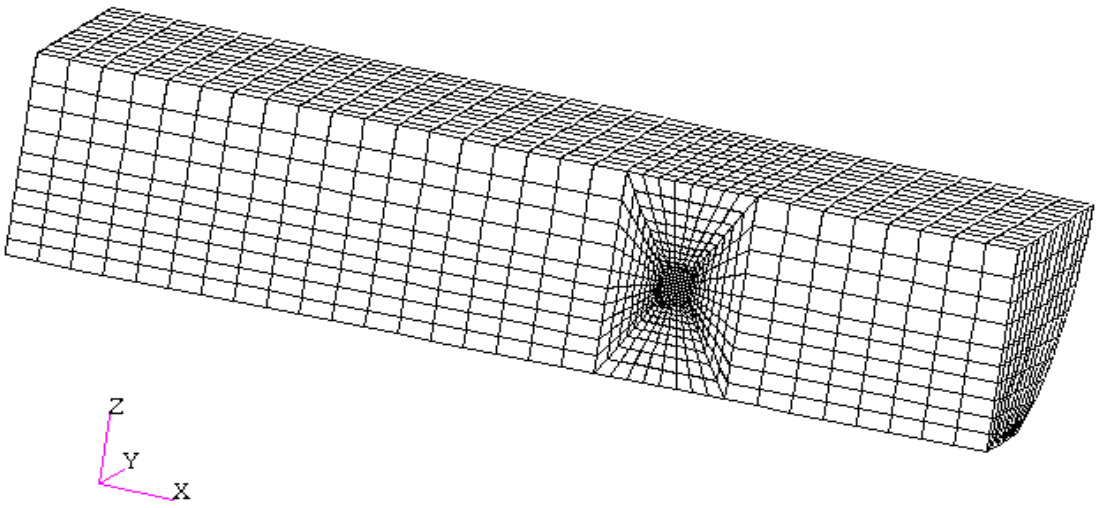

Figure 6. Eulerian Half Model Exposing the Core Section

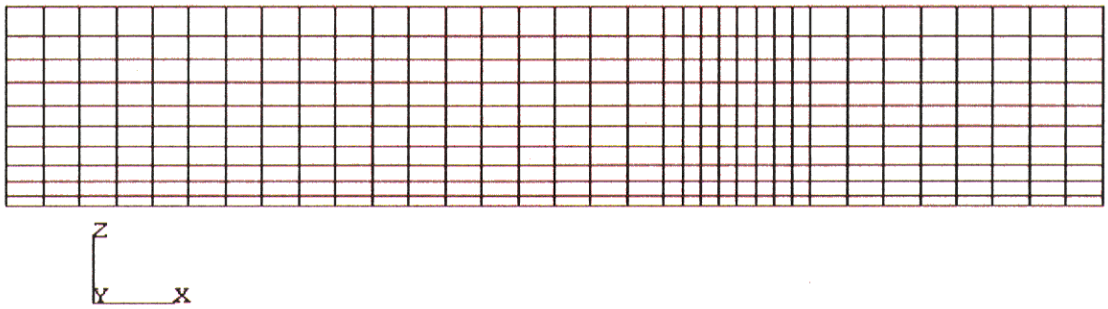

(a) MSC/DYTRAN Model I (charge at BS600)

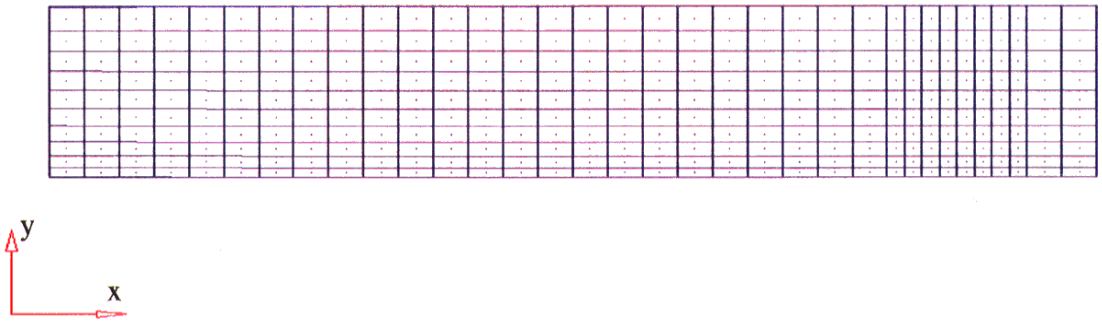

(b) MSC/DYTRAN Model II (charge at BS600F)

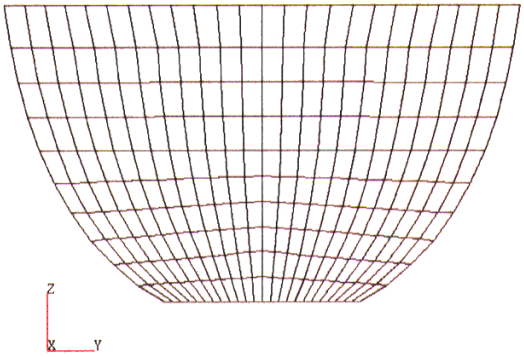

(c) Regular Transverse Cross-section (2-2)

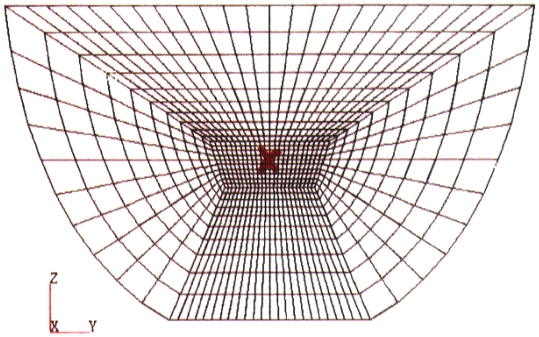

(d) Charge Location (1-1)

Figure 7. Cross-sections of the Euler Model

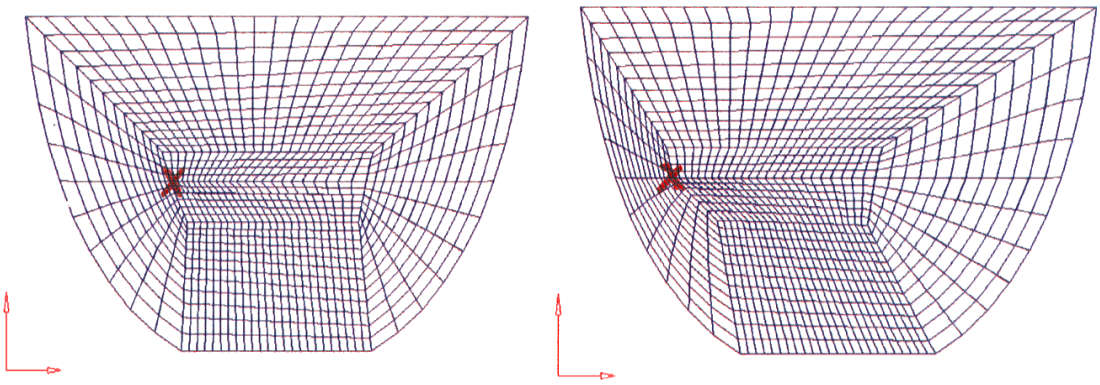

Figure 8. Transverse sections along (1-1)

4. Vulnerability Map - Results

Aircraft vulnerability and survivability are viewed as two distinct issues. The first issue is to examine the extent of damage of the structural components due to the internal explosion in flight (aircraft vulnerability). The second issue deals with the aircraft's ability to complete a flight profile and land safely at the nearest airport (aircraft survivability). Different strategies and methods are used to address the two issues.

MSC/DYTRAN global models are most appropriate to simulate the immediate effects of the explosion on the structure. MSC/NASTRAN global model is used to predict the behavior of the post explosion flight.

The following steps determine the vulnerability of the aircraft due to an in-flight explosion.

STEP 1: Determine the maximum allowable stresses for skins, frames and longerons based on their material definition and validation with the test matrix provided by the ALT-III series tests on the B-707 aircrafts [5]. The material allowable determined for the three main airframe components are 60 ksi for skins, and 80 ksi for frames and longerons.

STEP 2: Identify operating stresses on the forward fuselage for internal pressurization(8.6 psi) and 2.5 g load condition (worst case scenario) for the three components (skins, frames and longerons) - **Global MSC/NASTRAN static analysis.**

STEP 3: Perform a global MSC/DYTRAN analysis at a specific location and a known charge size. Compute stresses on skin, frames and longerons at various time intervals. Determine the maximum stress on all components for the given time range. - **Global MSC/DYTRAN fluid structure analysis**

STEP 4: Superimpose the operating stresses derived from STEP 2 on the stresses obtained at various time from the global MSC/DYTRAN analysis (STEP 3).

STEP 5: Identify elements in the global MSC/NASTRAN model that have exceeded the maximum allowable stresses computed in STEP 1.

Depending on the number of frames, longerons and skins identified as failed due to the internal explosion, a judgement can be reached whether the aircraft will survive the internal explosion. Steps 1 through 5 are performed for different charge sizes at the same location to determine the lowest charge size the aircraft structure can withstand to survive. The same procedure is then performed for different locations. By this method a vulnerability map can be constructed for the forward fuselage. In this paper a analysis matrix for six different locations is computed. At each of this locations the maximum charge size that the aircraft can withstand is computed. Consequently, the smallest charge size that can produce an aircraft “kill” is obtained and used to construct a vulnerability map.

The failure criteria for the frame and longerons were determined by the comparison of analytical predictions with those from the ALT-III test series. The percent increase to obtain the failure criteria for the frames from their material allowable was used to determine the failure stress criteria for the skin. The broken lines in Figure 9 show frames failed due to an explosion from a charge size 3 at location 1 at BS600 in the ALT-III test and visible to the naked eye, while the solid lines indicate frames whose maximum stresses under the same loading condition were above 80 ksi in the MSC/DYTRAN simulation. A good correlation between the MSC/DYTRAN analytical stress prediction and the test has helped to determine the failure stress criteria of 80,000 psi for frames and longerons, and 60,000 psi for the skin.

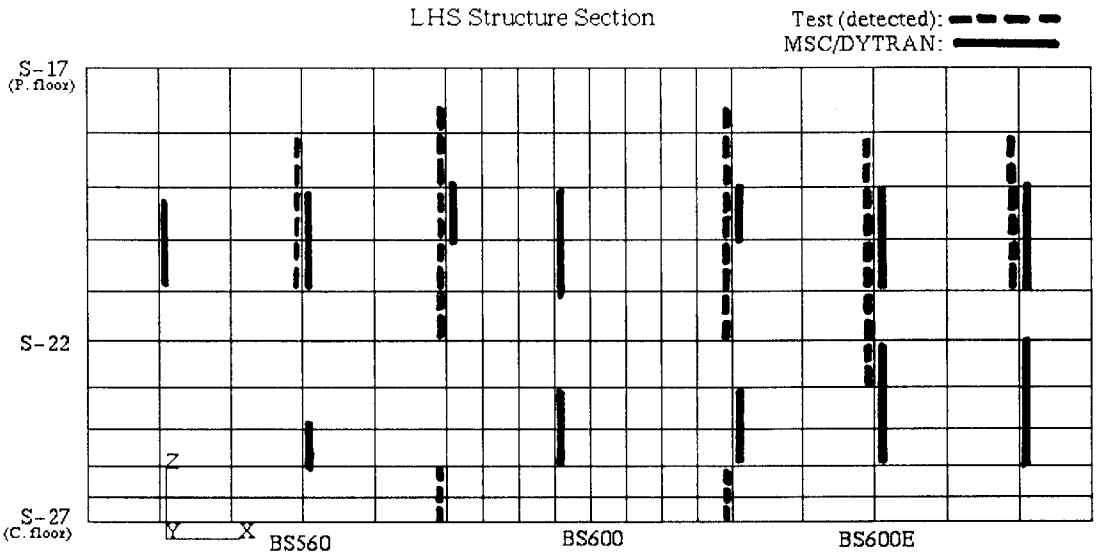

Figure 9. Comparison between test and analysis for determining the frame failure criteria

Once the failure criteria for the structural components was determined, the next step was to select a location (e.g. Location 1 at BS600) and run MSC/DYTRAN model for a given charge size (Step 3 in Page 15). Next. the stresses from the MSC/DYTRAN run were superimposed with the static stresses from MSC/NASTRAN (for the worst case flight condition) as outlined in Step 2. Failed elements in the global MSC/NASTRAN model were identified (Step 5). If the aircraft structure survived for the charge size depending on the number of failed components, the charge size was increased by one, and the procedure was repeated until the maximum charge size the air-craft structure can withstand was determined. The whole procedure was repeated to obtain the maximum charges at two body station locations (BS 600 and BS 600F), and at three transverse locations (Locations 1,2 & 3) for each of the body station locations. The results are compiled and shown in Figure 10 which constitutes a vulnerability map for the forward fuselage of the B-707 aircraft. The map shows the minimum charge size which results in an aircraft "kill" when the charge is detonated at the specified region. As the cargo door can be treated essentially invulnerable because of large mass and high stiffness, it was assumed in Figure 10 that the minimum charge size around the cargo door is a charge size higher than its counter-part on the other side of the aircraft centerline.

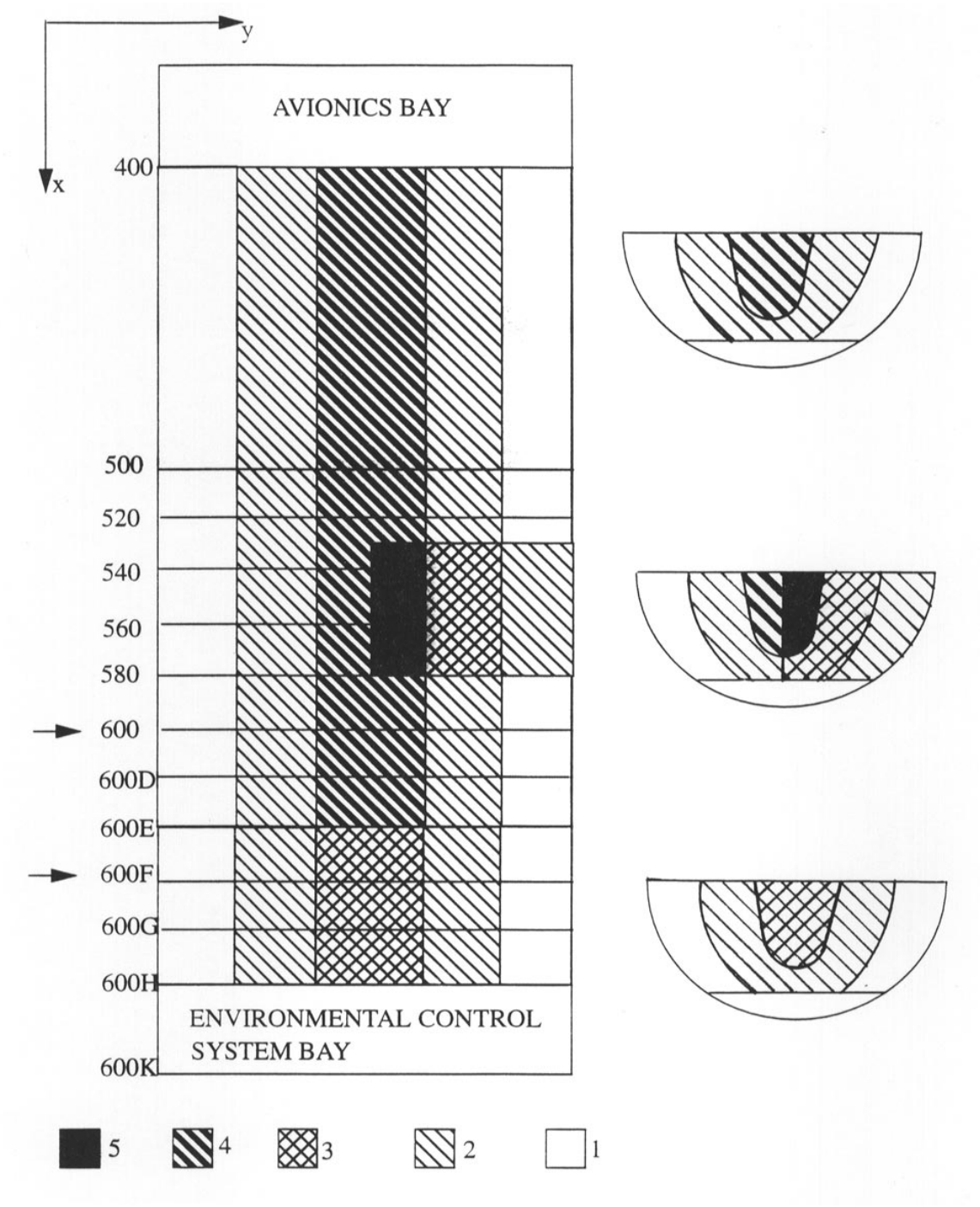

Figure 10. Vulnerability Map for the Forward Fuselage

5. Summary and Conclusions

An analytical method to construct a vulnerability map of a commercial aircraft is presented in this paper for internal explosions in the cargo bay. Two types of finite element models were constructed and used to draw the map. MSC/NASTRAN models were run to obtain a set of static stresses due to flight loading conditions, and MSC/DYTRAN models were used to compute time-varying stresses of all the structural components (frames, longerons and skins) when a known charge size is detonated at the specified locations. The failure criteria for the structural components were based on the ART-III test series. Presented also are steps to determine the vulnerability and survivability of an aircraft due to an in-flight explosion.

The concept outlined in the steps described in section 4 was applied to the forward fuselage of B-707 aircraft, and a vulnerability map of the aircraft structure was developed showing the minimum charge size required to produce an aircraft “kill”. Critical judgement was reached by the authors to determine what is considered as an aircraft “kill”. Skin breach was considered to be an immediate “kill” for the aircraft when a charge is placed at location 1. If the combination of frames (three full frame lengths - from passenger to cargo floor) and longerons (especially closer to the wing root) that failed was high, that too was considered as an aircraft structural “kill”. It is also to be noted that the vulnerability map developed in this effort is based on bare charges in unlined aircrafts. The vulnerability map provides a qualitative perspective of the vulnerable regions.

The map can be used to develop aircraft hardening strategies and to make commercial airplanes safer to the threat on internal explosions. The ultimate goal of this methodology would be to determine potential problems for an aircraft exposed to explosives while it is still on the drawing board.

References

1.Moon,Y.I., Bharatram, G., Schimmels, S.A. and Venkayya, V.B. “Vulnerability and Survivability Analysis of Aircraft Fuselage subjected to Internal Detonations,” MSC 1995 World Users’ Conference Proceedings, May 8-12, 1995

2.Moon,Y.I., Bharatram, G., Schimmels, S.A. and Venkayya, V.B. “Structural Analysis of B-707 Forward Fuselage with Internal Detonations,” WL-TR-95_XXXX, May 1995

3. “Fuselage Stress Analysis for 700-300 and -400 Series Airplane,” Vol.I,II,III, and IV, 1958, Boeing Airplane Co., Seattle, Wash.

4. MSC/DYTRAN - A 3D Code for Explicit Transient Dynamics. The MacNeal-Schwendler Corporation, Los Angeles, CA.

5. Schimmels, S.A., Flick, P.M., “Aircraft response test series III (ART-III). Data Analysis report: Volume 1 - Structures Test Results”, WL-TR-94-3159, October 1994.